Nonlinear Control of Propeller Induced Vibration

Wei Liu and Jie Pan

School of Mechanical and Chemical Engineering,

The University of Western Australia, Crawley WA 6009, Australia

ABSTRACT

Effective control of propeller induced vibration (PIV) is crucial not only in reducing underwater sound radiation from submarine hull structures, but also in noise analysis and control of unmanned underwater vehicles. The fact that PIV transmits along the same shafting which normally sustains enormous thrust means that the traditional insertion of elastic mounts between the thrust bearing housing and hall structure is not feasible, since the thrust transmission system will be softened. Thus active control (AC) and active & passive control (APC) techniques become attractive options for minimizing the dynamic PIV energy transmission into hull structures without globally softening the system.

This paper is a study of the dynamics of the active-controlled system with different configurations for understanding the controllability of this self-contained system where the dynamic energy will always be confined within the system without dissipation. A robust nonlinear backstepping method is then employed to implement the control strategy to handle the inherent nonlinear dynamics of the system. A double-side Active Magnetic Bearing (AMB) is utilized as the actuator, and proper switch functions are introduced to achieve differentiable vector sum of the forces from the two sides of the AMB. The parameter uncertainties and the unknown input of the PIV present another challenge which is addressed by using parameter estimators without bringing substantial complexity to the nonlinear controller. The effect of different design constants on the controller's performance is also discussed in detail. Simulation results show that the nonlinear active controller is stable and robust in minimizing the dynamic PIV energy transmitted into the hull structure. The results summarized in this paper also provide a basis for further development of more sophisticated active control systems for reducing PIV.

INTRODUCTION

Propeller induced vibration (PIV) is recognized to be the major source for sound radiation from submarines and similar structures at low frequencies. When submarines operate in deep water at low speed, the tonal component, mainly contributed by propeller induced vibration transmitted into hull structures, is dominant in the sound radiation under those operational conditions (Merz *et al*, 2007).

The dynamic excitation induced by a running propeller has received intense studies (Lewis, 1963). The asymmetry in the hull (Liu *et al*, 2010), protrusions of surfaces or shaft bearing struts result in a non-uniform wake field near the propeller, which then induces hydrodynamic excitations on the propeller shaft (Pan *et al*, 2002). A key feature of the propeller induced excitation is that it contains strong tonal components at the blade passing frequency (BPF) and its multiples.

Control of PIV is a challenging task. PIV transmits along the same shafting which normally sustains enormous thrust. Thus it is not feasible to insert elastic components into the transmission path for vibration control purpose. Realised this, Goodwin proposed resonance changer (RC) which uses a massive oil reservoir to absorb the propeller shaft vibration (Goodwin, 1960). Application of classical tuned mass absorbers was conducted by some researchers as well (Ojak 1984). However, the effectiveness of those methods is limited within narrow frequency band to which they are tuned.

Active control (AC) and active & passive control (APC) techniques are the two other options to minimize the dynamic PIV energy transmitted into hull structures without globally softening the shafting. Lewis & Allaire (1986) proposed active control for propeller induced oscillation. Baz *et al* (1988) utilized pneumatic servo-system to counteract the longitudinal vibration of a shaft. Dylejko *et al*, (2007) proposed adaptive control with a series of passive RC. Those studies however did not put too much attention on the reacting dynamic force transmitted into the receiving structures, which is critical for a self-contained system like a submarine.

This paper focuses on the pure active control where nonlinear backstepping control structures and active magnetic bearings are developed to address the dynamic energy received by the hull structures. The basis of this control structure is the system dynamics which indicates the controllability of the plant. Since pure active control scheme introduces no dissipation mechanism, the dynamic energy will be confined within the system and might cause instabilities. It is therefore necessary to examine the dynamics and controllability.

The control system includes a double-side active magnetic bearing (AMB) as an actuator. A special force distribution function is proposed to replace the switch function which is not differentiable. Also included in the system and analysis are the nonlinear propeller dynamics, thrust bearing oil film dynamics, the actuating dynamics, uncertainties of system parameters and unknown disturbances. One assumption used in this study is that when the propeller operates at a steady condition, the dominating tonal excitation is regarded as a time invariant stable excitation.

Section 4 presents the dynamics of the AMB actuator and a differentiable distribution function. Section 5 summarizes the controller design, and addressed the parameter uncertainties, unknown disturbance, also assessed the impact of the oil film dynamics. Section 6 gives the performance analysis with

different design constants. A summary of results and conclusions are presented in section 7.

SYSTEM MODELLING

A typical underwater vessel propulsion system can be illustrated as the Figure 1 which consists of propeller, shafting, thrust bearings, coupling and driving engine.

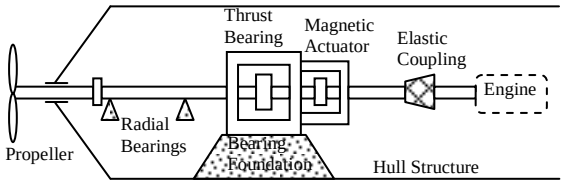

Figure 1 Typical underwater propulsion system

The running propeller simultaneously generates dynamic force and static thrust, which transmit together along the shaft into the bearing house through the bearing oil film. The dynamic force then transmits from the bearing house into the hull structure through the bearing foundation. Figure 2 gives the system model with assumption that the hull structure is rigid. The motions of the shaft mass (M_s) and bearing house mass (M_h) are described by equation (1).

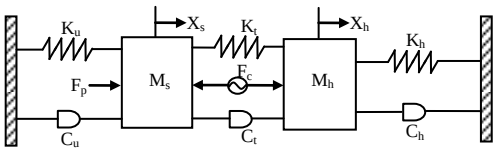

Figure 2 Mass-spring model of the propulsion system

$$\begin{cases} M_s\ddot{X}_s + (C_u + C_t)\dot{X}_s + (K_u + K_t)X_s - C_t\dot{X}_h - K_tX_h = F_p - F_c \\ M_h\ddot{X}_h + (C_h + C_t)\dot{X}_h + (K_h + K_t)X_h - C_t\dot{X}_s - K_tX_s = F_c \end{cases} \tag{1}$$

Where F_p and F_c are the PIV force and control force respectively, K_t,C_t are the oil film stiffness and damping of thrust bearing, K_h,C_h are the stiffness and damping of bearing house and K_u,C_u are the un-modelled system damping and stiffness, including couplings, friction of radial bearing, hydrodynamic damping of the propeller and internal damping of shaft. X_s and X_h are the displacement of the shaft and bearing house.

Define the following state space variables,

$$x_1 = X_h\,; x_2 = \dot{X}_h\,; x_3 = X_s\,; x_4 = \dot{X}_s \tag{2}$$

We can write (1) into the state space and output equations.

$$\begin{cases} \dot{x}_1 = x_2 \\ \dot{x}_2 = -(\theta_{21} + \theta_{23})x_1 - (\theta_{22} + \theta_{24})x_2 + \theta_{21}x_3 + \theta_{22}x_4 + F_c \\ \dot{x}_3 = x_4 \\ \dot{x}_4 = r\theta_{21}x_1 + r\theta_{22}x_2 - (r\theta_{21} + \theta_{41})x_3 - (r\theta_{22} + \theta_{42})x_4 + rF_c + \dfrac{F_p}{M_s} \end{cases}$$

$$\mathbf{y} = [x_1 \quad x_2]^T \tag{3}$$

With

$$\theta_{21} = \frac{K_t}{M_h}, \theta_{22} = \frac{C_t}{M_h}, \theta_{23} = \frac{K_h}{M_h}, \theta_{24} = \frac{C_h}{M_h}, \theta_{41} = \frac{K_u}{M_s}, \theta_{42} = \frac{C_u}{M_s}, r = \frac{M_h}{M_s}$$

The dynamic force F_c generated by the AMB's interacts with the shaft will act on the bearing house to cancel the primary PIV excitation. The goal is to tune the control force F_c to cut off the dynamic energy flowing into the hull structure, i.e. to regulate the thrust bearing house response (x_1, x_2) to zero while at the same time stabilize the shaft response (x_3, x_4).

ANALYSIS OF SYSTEM DYNAMICS

Active control system will have the vibratory energy confined in the system since there is no energy dissipation mechanism introduced. In this application, if the control was successful, the dynamic energy will stop flowing into the hull structure; however, it will then flow into the shaft. Now the question is how it is going to affect the stability of the system?

3.1 Zero dynamics

The states of the shaft (x_3, x_4) are not observable from the output $\boldsymbol{y}$ under the control scheme. They are the hiding dynamics or zero dynamics which should be addressed in the stability analysis of the close loop system. Let's apply a feedback control to the plant, where $k_{1,2}$ are design constants.

$$F_c = (\theta_{21} + \theta_{23} - 1 - k_1 \cdot k_2)x_1 + (\theta_{22} + \theta_{24} - k_1 - k_2)x_2 - \theta_{21}x_3 - \theta_{22}x_4 \tag{4}$$

The close loop hiding dynamics (x_3, x_4) can be expressed as:

$$\begin{cases} \dot{x}_3 = x_4, \\ \dot{x}_4 = -r\theta_{23}x_1 - r\theta_{24}x_2 - \theta_{41}x_3 - \theta_{42}x_4 - x_1 - k_1x_2 \\ \quad -k_2(x_2 + k_1x_1) + \dfrac{F_p}{M_s} \end{cases} \tag{5}$$

When the output $\boldsymbol{y} \to 0$, then $x_1 \to 0$, $x_2 \to 0$. Substitute it into the above equations, we have

$$\begin{Bmatrix} \dot{x}_3 \\ \dot{x}_4 \end{Bmatrix} = \begin{bmatrix} 0 & 1 \\ -\theta_{41} & -\theta_{42} \end{bmatrix} \begin{Bmatrix} x_3 \\ x_4 \end{Bmatrix} + \begin{bmatrix} 0 \\ 1 \end{bmatrix} \cdot \frac{F_p}{M_s} \tag{6}$$

Since θ_{41}, θ_{42} are both positive, based on linear control theory, the matrix is Hurwitz. Because F_p is a bounded input all the time, the states (x_3, x_4) are therefore bounded all the time. According to stability theories (Kristic *et al*, 1995), the system is an ISS (Input to Output Stability) stable system.

3.2 Shaft response under different system configurations

Although the system is ISS stable, we are also interested in how the shaft response is going to change after the energy flows in. Whether it's going to increase or decrease, and to what extent or under what circumstance? Since this dynamics strongly depends on system configurations, we examined three different scenarios of the system with different structural configurations.

*Scenario I: I*s the shaft-thrust bearing sub-system a complex stiffness ($|K_t+j\omega C_t|$) dominating or Mass ($|-\omega^2 M_s|$) dominating system? From the energy point of view, the ratio of the oil film's complex stiffness $|K_t+j\omega C_t|$ to the shafting mass $|-\omega^2 M_s|$ shows the percentage of energy transmitted into the bearing house and hull structure, and that trapped in the shaft.

*Scenario II: I*s the complex stiffness of the thrust bearing foundation $|K_h+j\omega C_h|$ relatively stiff or relatively soft?

*Scenario III: I*s the un-modelled system complex stiffness $|K_u+j\omega C_u|$ relatively great or small?

We use the transfer functions for the dynamics analysis.

$$\begin{cases} \dfrac{x_1}{F_p} = \dfrac{C_t \cdot s + K_t}{D(\bullet)} \\ \dfrac{x_3}{F_p} = \dfrac{M_h \cdot s^2 + (C_t + C_h)\cdot s + (K_t + K_h)}{D(\bullet)} \\ D(\bullet) = M_s M_h \cdot s^4 + (M_s M_t + M_s C_h + M_h C_t + M_h C_u)\cdot s^3 \\ \quad + (M_s K_t + M_s K_h + C_t C_h + C_t C_u + C_u C_h + M_h K_t \\ \quad + M_h k_u)\cdot s^2 + (C_t K_h + C_u K_t + C_u K_h + C_t K_u + C_h K_t \\ \quad + C_h K_u)\cdot s + (K_t K_h + K_u K_t + K_u K_h) \end{cases} \tag{7}$$

The shaft responses before and after control were simulated under the three configuration scenarios where the parameters vary from 0.01 to 100 times of their nominal configuration as listed in table 1, which is similar to the one from Lewis and Allaire (Lewis & Allaire, 1986).

Table 1 Nominal parameters used for simulations

Parameters	*Description*	*Nominal value*
f	PIV frequency, assume shaft revolution is 240rpm and 5blades propeller	20 Hz
M_s	Mass of the shaft	2e4 kg
K_t	Oil film stiffness	1e9 N/m
C_t	Oil film damping	1e6 Ns/m
M_h	Mass of bearing house	1e4 kg
K_h	Bearing house stiffness	9e9 N/m
C_h	Bearing house damping	1e6 Ns/m
K_u	Un-modelled stiffness	1e6 N/m
C_u	Un-modelled damping	1e6 Ns/m

Figure 3 is an example mapping plot showing the change of the shaft responses after the control under different configuration scenario I & II. The change ratio is in dB, where the negative value means the shaft response decreases after the control, the positive value means increases after the control, and the zero value indicates no change of shaft response. The mapping is separated by the zero value curves into response increasing area and response decreasing area.

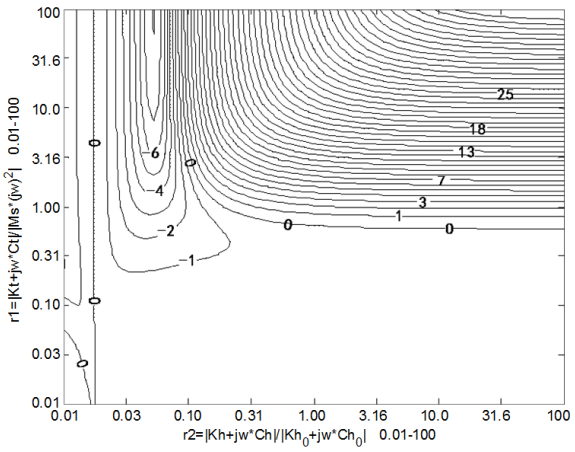

Figure 3 Log ratio of shaft response after control to shaft response before control, under scenario I & scenario II.

3.3 Observations and comments

a) The plant is controllable; the system is an ISS (Input to Output Stability) stable system.

b) The impact of the diverted energy on the shaft responses depends on the configurations of the system. For those cases fall in the increasing area, the increased response might hit the physical bound of the AMB air gap limit.

c) There are possibilities that the shaft responses being attenuated as well after the control.

AMB ACTUATOR

Actuator is a critical part of the active control scheme. The capacity of the actuator determines the performance of the control system; on the other hand, the dynamics of the actuator also greatly affect the design of the controller. Various types of conventional actuators like inertial, hydraulic and pneumatic ones, and non-conventional actuators like shape memory alloys, piezo-ceramics, mechano-chemical polymer have been widely used to control structures vibration and sound radiation (Hansen & Snyder 1997).

To control the propeller induced vibration, there are several special requirements for actuating. First, the actuator should be able to apply forces between a rotating shaft and static bearing house. Second, the actuator should not introduce new path of transmitting reaction force into hull structures. Third, the actuator should be capable of generating relatively large forces with compact size. Due to these requirements, we proposed Active Magnetic Bearing (AMB) as the actuator in this research.

4.1 Force-voltage model of a single-side AMB

A double-side AMB consisting of two mechanically jointed single AMBs are proposed as Figure 4. Separately controlled AMB1 and AMB2 will only generate attractive force.

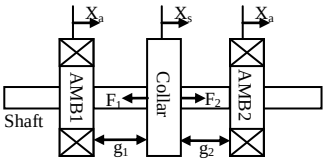

Figure 4 Double AMB consists of two single AMBs

For the single AMB on each side of the collar, the relations between electrical control input and the forces generated can be expressed as (Schweitzer *et al*, 1994).

$$\begin{aligned} F_q\left(X_a, X_s, i_q\right) &= -\frac{\mu_0 A_g N^2}{4 g_q^2\left(X_a, X_s\right)} i_q^2 \\ R_q i_q &= V_q - \left(L_q \frac{di_q}{dt} + i_q \frac{dL_q}{dg_q}\frac{dg_q}{dt} \right) \\ g_q\left(X_a, X_s\right) &= g_{0q} \pm \left(X_a - X_s\right), \quad q = 1,2 \end{aligned} \tag{8}$$

Where X_a is the displacement of AMB which is mounted onto the bearing house and thus we have X_a=X_h. μ_0 is the permeability of the air, N is the turns of AMB coil, A_g is the cross section area of flux path. R_q and L_q are the resistance and inductance of the coil, g_q is the air gap and g_{0q} is the initial air gap. i_q and V_q are the control current and control voltage respectively.

The following physical restrictions apply in this study:

$$g_q\left(X_a, X_s\right) > 0 \; and \sum_{q=1,2} g_q\left(X_a, X_s\right) = \text{Constant} \tag{9}$$

The control force of the double-side AMB will be the combination of the two single attractive forces generated by AMB1 and AMB2, in the form of vector sum:

$$F_c = \sum_{q=1,2} \vec{F}_q \tag{10}$$

4.2 Force distribution model of the double-side AMB

For the double-side AMB in Figure 4, the two attractive forces generated are always opposite and tend to cancel each other to some degree. To maximize the capacity of the combined control force F_c, the two single forces need to satisfy the following combination. Assume F_2 is in positive direction.

$$\begin{cases} \text{if } F_c > 0 \quad F_1 = 0,\ F_2 = F_c \\ \text{if } F_c < 0 \quad F_1 = F_c,\ F_2 = 0 \end{cases} \tag{11}$$

This force distribution function is an ideal case of the force switching between the two single-side AMBs. To design the control voltage $u_{1,2}$ later, we need to use the derivative of the control force F_c. Noticing that equation (11) is not differentiable, we proposed a replacement force distribution function as the following and illustrated in Figure 5:

$$\begin{cases} F_1 = \frac{1}{2}(F_c - \sqrt{F_c^2 + \gamma_0^2}) \\ F_2 = \frac{1}{2}(F_c + \sqrt{F_c^2 + \gamma_0^2}) \end{cases}, \quad \gamma_0 \text{ is a small design constant} \tag{12}$$

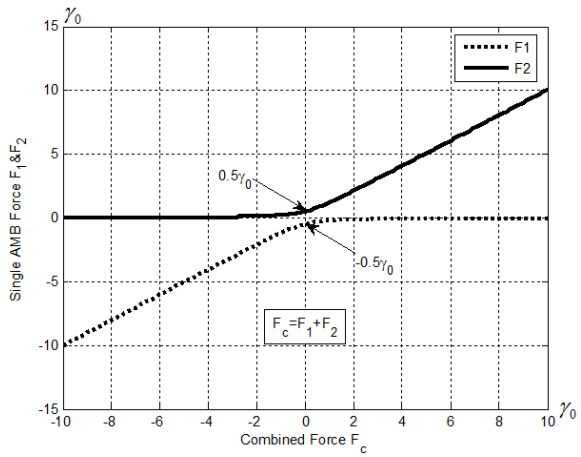

Figure 5 Force distribution function for double-side AMB

The following properties are obvious with function (12):

a) F_c is differentiable since $F_1 + F_2 = F_c$ at any time;

b) when $F_c < 0$, $F_1 \approx F_c, F_2 \approx 0^+$, $\lim_{F_c \to -\infty} F_1 = F_c$, $\lim_{F_c \to -\infty} F_2 = 0$;

c) when $F_c > 0$ $F_1 \approx 0^-, F_2 \approx F_c$, $\lim_{F_c \to \infty} F_1 = 0$, $\lim_{F_c \to \infty} F_2 = F_c$;

d) when $F_c = 0$, $F_1 = -\frac{1}{2}\gamma_0, F_2 = \frac{1}{2}\gamma_0$.

CONTROLLER DESIGN

The complete system model can be combined from the plant and the actuator as the following state space description equation (13), where g_0 is the initial air gap of one AMB; Constant C_{tgap} is the total gap of the two sides. dL/dg is the derivative of the inductance to air gap which is assumed to be zero for simplification. $u_{1,2}$ is the control voltage for the two single AMBs.

$$\begin{cases} \dot{x}_1 = x_2 \\ \dot{x}_2 = -(\theta_{21} + \theta_{23})x_1 - (\theta_{22} + \theta_{24})x_2 + \theta_{21}x_3 + \theta_{22}x_4 \\ \quad - \theta_{25}\dfrac{i_1^2}{(g_{01} + x_3 - x_1)^2} + \theta_{25}\dfrac{i_2^2}{(g_{02} + x_1 - x_3)^2} \\ \dot{x}_3 = x_4 \\ \dot{x}_4 = r\theta_{21}x_1 + r\theta_{22}x_2 - (r\theta_{21} + \theta_{41})x_3 - (r\theta_{22} + \theta_{42})x_4 \\ \quad + r\theta_{25}\dfrac{i_1^2}{(g_{01} + x_3 - x_1)^2} - r\theta_{25}\dfrac{i_2^2}{(g_{02} + x_1 - x_3)^2} + \dfrac{F_p}{M_s} \\ \dot{i}_1 = \theta_{51}i_1 + u_1 \\ \dot{i}_2 = \theta_{61}i_2 + u_2 \end{cases}$$

$$y = [x_1 \quad x_2]^T$$

$$\theta_{21} = \frac{K_t}{M_h}, \theta_{22} = \frac{C_t}{M_h}, \theta_{23} = \frac{K_h}{M_h}, \theta_{24} = \frac{C_h}{M_h}, \theta_{25} = \frac{\mu_0 A_g N^2}{4M_h},$$

$$\theta_{41} = \frac{K_u}{M_s}, \theta_{42} = \frac{C_u}{M_s}, g_{01} = g_0, g_{02} = C_{tgap} - g_0, r = \frac{M_h}{M_s}, u_1 = \frac{V_1}{L_1},$$

$$u_2 = \frac{V_2}{L_2}, \theta_{51} = \frac{1}{L_1}(-R_1 + \frac{dL_1}{dg_1} \cdot \frac{dg_1}{dt}), \theta_{61} = \frac{1}{L_2}(-R_2 + \frac{dL_2}{dg_2} \cdot \frac{dg_2}{dt}) \tag{13}$$

System Characteristics

The following issues characterize the model and need to be addressed, a) Nonlinearity of AMB dynamics and oil film dynamics; b) Parameters uncertainties. For a real plant, the dynamic properties K_t, C_t, K_h, C_h, K_u and C_u which correspond to θ_{21}, θ_{22}, θ_{23}, θ_{24}, θ_{41} and θ_{42} in Equation (13) are all unknown; c) Unknown disturbance. The magnitude of propeller induced vibration is very difficult to obtain in practice.

5.1 Nonlinear backstepping controller

To control the nonlinear dynamics we employed Backstepping technique which is flexible and capable of robustly accounting for fast time variations of modelling errors and external disturbances (Kristic *et al*, 1995). Equation (15)-(16) gives the expression of the nonlinear controller. The controller works towards regulating the derivative of the following Lyapunov energy function (14) to negative.

$$V = \frac{1}{2}[z_1 \quad z_2 \quad z_3 \quad z_4]\begin{bmatrix} -k_1 & 0 & 0 & 0 \\ 0 & -k_2 & 0 & 0 \\ 0 & 0 & -k_3 & 0 \\ 0 & 0 & 0 & -k_4 \end{bmatrix}[z_1 \quad z_2 \quad z_3 \quad z_4]^T \tag{14}$$

Detailed results of the controller design and stability proof will be published separately.

$$\begin{aligned} u_1 &= -k_3 z_3 - \theta_{51}i_1 + \theta_{25}\frac{z_2(z_3 + 2\alpha_{21})}{(g_{01} + x_3 - x_1)^2} - \frac{x_2}{\sqrt{2\theta_{25}}}(\sqrt{\sqrt{F_\alpha^2 + \gamma_0^2} - F_\alpha}) \\ &+ \frac{x_4}{\sqrt{2\theta_{25}}}(\sqrt{\sqrt{F_\alpha^2 + \gamma_0^2} - F_\alpha}) + \frac{1}{\sqrt{2\theta_{25}}}(g_{01} + x_3 - x_1) \\ &\times \frac{1}{2\sqrt{\sqrt{F_\alpha^2 + \gamma_0^2} - F_\alpha}} \cdot (\frac{F_\alpha}{\sqrt{F_\alpha^2 + \gamma_0^2}} - 1) \cdot \{(\theta_{21} + \theta_{23} - 1 - k_1 k_2)x_2 \\ &+ (\theta_{22} + \theta_{24} - k_1 - k_2) \cdot [-(\theta_{21} + \theta_{23})x_1 - (\theta_{22} + \theta_{24})x_2 + \theta_{21}x_3 \\ &+ \theta_{22}x_4 - \theta_{25}\frac{i_1^2}{(g_{01} + x_3 - x_1)^2} + \theta_{25}\frac{i_2^2}{(g_{02} + x_1 - x_3)^2}] - \theta_{21}x_4 \\ &- \theta_{22}[r\theta_{21}x_1 + r\theta_{22}x_2 - (r\theta_{21} + \theta_{41})x_3 - (r\theta_{22} + \theta_{42})x_4 \\ &+ r\theta_{25}\frac{i_1^2}{(g_{01} + x_3 - x_1)^2} - r\theta_{25}\frac{i_2^2}{(g_{02} + x_1 - x_3)^2} + \frac{F_p}{M_s}]\} \end{aligned} \tag{15}$$

$$
\begin{aligned}
u_2 &= -k_4 z_4 - \theta_{61} i_2 - \theta_{25}\frac{z_2(z_4+2\alpha_{22})}{(g_{02}+x_1-x_3)^2} + \frac{x_2}{\sqrt{2\theta_{25}}}\left(\sqrt{\sqrt{F_\alpha^2+\gamma_0^2}+F_\alpha}\right) \\
&- \frac{x_4}{\sqrt{2\theta_{25}}}\left(\sqrt{\sqrt{F_\alpha^2+\gamma_0^2}+F_\alpha}\right) + \frac{1}{\sqrt{2\theta_{25}}}(g_{02}+x_1-x_3) \\
&\times \frac{1}{2\sqrt{\sqrt{F_\alpha^2+\gamma_0^2}+F_\alpha}} \cdot \left(\frac{F_\alpha}{\sqrt{F_\alpha^2+\gamma_0^2}}+1\right) \cdot \{(\theta_{21}+\theta_{23}-1-k_1k_2)x_2 \\
&+ (\theta_{22}+\theta_{24}-k_1-k_2)\cdot[-(\theta_{21}+\theta_{23})x_1 - (\theta_{22}+\theta_{24})x_2 + \theta_{21}x_3 \\
&+ \theta_{22}x_4 - \theta_{25}\frac{i_1^2}{(g_{01}+x_3-x_1)^2} + \theta_{25}\frac{i_2^2}{(g_{02}+x_1-x_3)^2}] - \theta_{21}x_4 \\
&- \theta_{22}[r\theta_{21}x_1 + r\theta_{22}x_2 - (r\theta_{21}+\theta_{41})x_3 - (r\theta_{22}+\theta_{42})x_4 \\
&+ r\theta_{25}\frac{i_1^2}{(g_{01}+x_3-x_1)^2} - r\theta_{25}\frac{i_2^2}{(g_{02}+x_1-x_3)^2} + \frac{F_p}{M_s}]\}
\end{aligned}
\tag{16}
$$

Together with the plant parameters as table 1, table2 listing AMB with capacity of generating up to 5% static thrust force was used for the simulations of the controller.

Table 2 Parameters used for the nonlinear controller

Parameters	*Description*	*Nominal value*
N	AMB coil turns	100
A_g	Cross section area of flux path	0.25 m2
μ_0	Permeability of air	$4\pi\times10^{-7}$ H/m
g_{01}	Initial air gap of AMB1	1e-3 m
g_{02}	Initial air gap of AMB2	1e-3 m
R_1	Resistance of AMB1	1 Ω
R_2	Resistance of AMB2	1 Ω
L_1	Inductance of AMB1 $=(\mu_0 A_g N^{2)}/(2g_{01})$	H
L_2	Inductance of AMB1 $=(\mu_0 A_g N^{2)}/(2g_{02})$	H
γ_0	Design constant of the force distribution function	0.1
F_p	Propeller excitation, 5% thrust	20sin(2πf) kN
$k_{1,2}$	Design constant $k_1=k_2=350$	N/A
$k_{3,4}$	Design constant $k_3=k_4=200$	N/A

Figure 6 shows the system responses; Figure 7 shows the control currents of AMBs. Control is on at the 10th seconds.

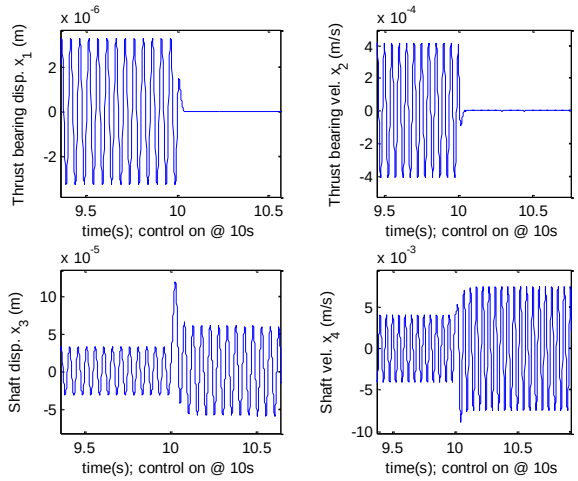

Figure 6 Bearing house response *(x_1, x_2)* and shaft response *(x_3, x_4)* under the nonlinear control; the controller is on at 10s

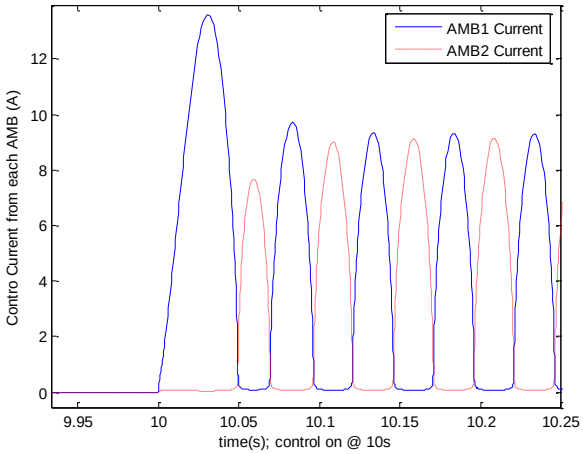

Figure 7 The control current from each AMB

Observations and comments

a) After the control is applied, the bearing house response (x_1, x_2) converges to zero rapidly, while the shaft response increases but is physically bounded. The force generated by a single-side AMB never reaches zero due to the introduction of the constant γ_0 in the force distribution function.

b) After a transient period, the control current from the two AMBs are almost the same, the peaks appear alternatively.

5.2 Uncertainty of system parameters

In section 5.1, the control design assumes all parameters are known which is not true in practice. The dynamic properties K_t, C_t, K_h, C_h, K_u *and* C_u which correspond to θ_{21}, θ_{22}, θ_{23}, θ_{24}, θ_{41} and θ_{42} in Equation (13) are also practically unknown.

Define $\theta_{21}^*, \theta_{22}^*, \theta_{23}^*, \theta_{24}^*, \theta_{41}^*, \theta_{42}^*$ as the estimations for the unknowns. A Lyapunov method based estimator is developed with the adaptive laws as the following:

$$
\begin{aligned}
\dot{\theta}_{21}^* &= \gamma_1(-x_1 z_2 + x_3 z_2) \\
\dot{\theta}_{22}^* &= \gamma_2(-x_2 z_2 + x_4 z_2) \\
\dot{\theta}_{23}^* &= -\gamma_3 x_1 z_2 \\
\dot{\theta}_{24}^* &= -\gamma_4 x_2 z_2, \quad \gamma_1 \sim \gamma_4 \text{ are the design constants}
\end{aligned}
\tag{17}
$$

The above estimations are however the over parameterization estimation structure. They will only be used as the interim virtual control (Kristic *et al*, 1995).

Based on the virtual control, we define new estimations as $\hat{\theta}_{21}, \hat{\theta}_{22}, \hat{\theta}_{23}, \hat{\theta}_{24}, \hat{\theta}_{41}, \hat{\theta}_{42}$. By regulating the derivative of the new Lyapunov function with time to negative, the adaptive laws for the system parameters are obtained as equation (18).

The estimator was simulated with $k_1=k_2=800$; $k_3=k_4=200$; $\gamma_1=1e10$; $\gamma_2=1e6$; $\gamma_3=\gamma_4=1e5$; $\beta_1=1e7$; $\beta_2=\beta_3=\beta_4=\beta_5=\beta_6=1e5$, and initial values of $\theta_{21}^* = 1e4$, $\theta_{22}^* = 1e1$, $\theta_{23}^* = 5e5$, $\theta_{24}^* = 5e1$, $\hat{\theta}_{21} = 1e4, \hat{\theta}_{22} = 1e1, \hat{\theta}_{23} = 5e5, \hat{\theta}_{24} = 5e1, \hat{\theta}_{41} = \hat{\theta}_{42} = 25$. Figure 8 shows the system responses with the parameter estimator in presence. Figure 9 shows the convergence of the unknown parameters $\hat{\theta}_{21}, \hat{\theta}_{22}, \hat{\theta}_{23}, \hat{\theta}_{24}$.

$$\dot{\hat{\theta}}_{21} = -\beta_1 \begin{Bmatrix} z_3[\xi_1(\square) f_2(\square) + r\xi_1(\square)\theta^*_{22}](x_3 - x_1) \\ + z_4[\xi_2(\square) f_2(\square) + r\xi_2(\square)\theta^*_{22}](x_3 - x_1) \end{Bmatrix}$$

$$\dot{\hat{\theta}}_{22} = -\beta_2 \begin{Bmatrix} z_3[\xi_1(\square) f_2(\square) + r\xi_1(\square)\theta^*_{22}](x_4 - x_2) \\ + z_4[\xi_2(\square) f_2(\square) + r\xi_2(\square)\theta^*_{22}](x_4 - x_2) \end{Bmatrix}$$

$$\dot{\hat{\theta}}_{23} = \beta_3 \{ z_3[\xi_1(\square) f_2(\square)]x_1 + z_4[\xi_2(\square) f_2(\square)]x_1 \}$$

$$\dot{\hat{\theta}}_{24} = \beta_4 \{ z_3[\xi_1(\square) f_2(\square)]x_2 + z_4[\xi_2(\square) f_2(\square)]x_2 \}$$

$$\dot{\hat{\theta}}_{41} = -\beta_5 \{ z_3[\xi_1(\square)\theta^*_{22}]x_3 + z_4[\xi_2(\square)\theta^*_{22}]x_3 \}$$

$$\dot{\hat{\theta}}_{42} = -\beta_6 \{ z_3[\xi_1(\square)\theta^*_{22}]x_4 + z_4[\xi_2(\square)\theta^*_{22}]x_4 \}$$

where $\beta_1 \sim \beta_6$ are the design constants, and

$$\phi_1(\square) = \frac{1}{\sqrt{2\theta_{25}}}\left(\sqrt{\sqrt{F_\alpha^2 + \gamma_0^2} - F_\alpha}\right),$$

$$\phi_2(\square) = \frac{1}{\sqrt{2\theta_{25}}}\left(\sqrt{\sqrt{F_\alpha^2 + \gamma_0^2} + F_\alpha}\right),$$

$$f_1(\square) = \theta^*_{21} + \theta^*_{23} - 1 - k_1 k_2, \; f_2(\square) = \theta^*_{22} + \theta^*_{24} - k_1 - k_2$$

$$\xi_1(\square) = \frac{1}{\sqrt{2\theta_{25}}}(g_{01} + x_3 - x_1) \cdot \frac{1}{2\sqrt{\sqrt{F_\alpha^2 + \gamma_0^2} - F_\alpha}} \cdot \left(\frac{F_\alpha}{\sqrt{F_\alpha^2 + \gamma_0^2}} - 1\right)$$

$$\xi_2(\square) = \frac{1}{\sqrt{2\theta_{25}}}(g_{02} + x_1 - x_3) \cdot \frac{1}{2\sqrt{\sqrt{F_\alpha^2 + \gamma_0^2} + F_\alpha}} \cdot \left(\frac{F_\alpha}{\sqrt{F_\alpha^2 + \gamma_0^2}} + 1\right)$$

(18)

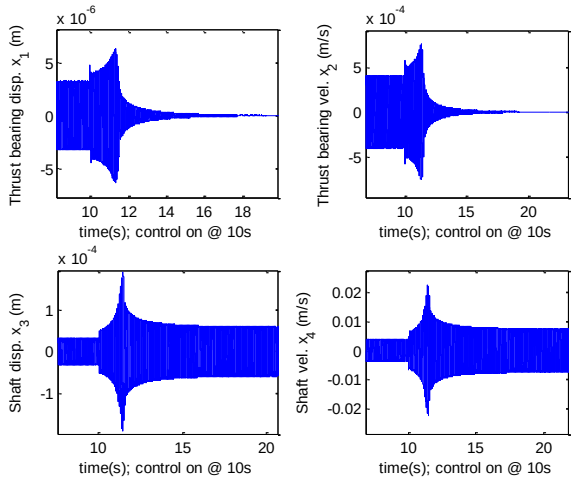

Figure 8 Bearing house response (x_1, x_2) and shaft response (x_3, x_4) under the nonlinear control with parameter estimators

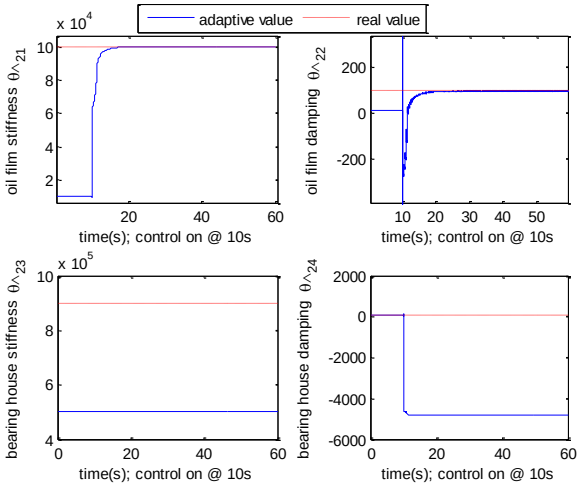

Figure 9 Performance of the estimator for $\hat{\theta}_{21}, \hat{\theta}_{22}, \hat{\theta}_{23}, \hat{\theta}_{24}$; $\hat{\theta}_{21}, \hat{\theta}_{22}$ converged to true values, control goals achieved

Observations and comments

a) The over-parameterized estimator works successfully with the controller to regulate the bearing house response (x_1, x_2).

b) The estimator has an obvious negative impact on the transient performance of the controller.

c) Not all the unknowns converged to their true value due to inadequate persistent exciting condition. However, the discrepancy of the converged constant and the true value does not affect the controller in achieving the goals.

5.3 Unknown Disturbance

In equations (15)-(16) for the controller u_1, u_2, the disturbance F_p is normally regarded as unknown. The reason is that it is extremely difficult to obtain accurate theoretical model to describe propeller induced dynamic force. However, at steady operational condition, the tone dominated excitation at the BPF can be modelled as, where n is the shaft speed, N_b is the blade number, $\emptyset_0$ is the initial phase, C_n is an amplitude constant and $f(n)$is a nonlinear amplitude function.

$$F_p = C_n \cdot f(n) \cdot \sin\left(\frac{2\pi n N_b}{60} t + \phi_0\right) \tag{19}$$

In this case, $C_n \cdot f(n)$ can be regarded as a combined unknown constant. However, the unknown initial phase ϕ_0 is very difficult to estimate since it is in the nonlinear time variable term. However for feedback control, we do not have to estimate the disturbance. Nevertheless, using the second and the fourth equation from equation (3) the following can be obtained:

$$F_p = M_s(r\dot{x}_2 + \dot{x}_4 + r\theta_{23}x_1 + r\theta_{24}x_2 + \theta_{41}x_3 + \theta_{42}x_4) \tag{20}$$

Notice that the PIV is mainly tonal component whose frequency is easily available. With equation (19), we have:

$$\dot{x}_2 = \ddot{x}_1 = -\left(\frac{2\pi n N_b}{60}\right)^2 x_1, \; \dot{x}_4 = \ddot{x}_3 = -\left(\frac{2\pi n N_b}{60}\right)^2 x_3 \tag{21}$$

Substitute equation (21) into equation (20), we have the steady state estimate of the propeller force based system states and shaft speed:

$$F_p = M_s \begin{Bmatrix} \left[r\theta_{23} - \left(\frac{2\pi n N_b}{60}\right)^2\right] x_1 + r\theta_{24}x_2 \\ + \left[\theta_{41} - \left(\frac{2\pi n N_b}{60}\right)^2\right] x_3 + \theta_{42}x_4) \end{Bmatrix}. \tag{22}$$

5.4 Oil film dynamics

The dynamics of the oil film of the thrust bearings are very complicated. The stiffness and damping of the oil film are normally nonlinear functions of the thrust load and the oil film thickness. In this application, at a specific steady operational condition, the thrust load can be regarded as quasi-constant. With regarding to the oil film thickness, the dimensionless stiffness and damping (Storteig Eskild 1999) can be employed to roughly give the expression of the stiffness and damping in terms of oil film thickness as equation (23), where B, L are the thrust bearing geometry, U is the relative speed difference, h_0 is the initial thickness under static thrust

load, μ is the fluid viscosity, x_h and x_s are the bearing house displacement and shaft displacement respectively; Also in the equation $K_t^* = \bar{K}_t \mu U B L^2$, $C_t^* = \bar{C}_t \mu B L^3$.

$$K_t = \frac{\bar{K}_t \mu U B L^2}{h^3} = \frac{K_t^*}{h^3} = \frac{K_t^*}{(h_0 + f(x_h, x_s))^3}$$
$$C_t = \frac{\bar{C}_t \mu B L^3}{h^3} = \frac{C_t^*}{h^3} = \frac{C_t^*}{(h_0 + f(x_h, x_s))^3} \quad (23)$$

By using the definition of stiffness K_t

$$K_t = \frac{dF}{dh} = \frac{dF}{d(h_0 + f(x_h, x_s))}, \quad (24)$$

Equation (23) and integration, we have

$$F[h_0 + f(x_h, x_s)]^2 = \text{constant} \quad (25)$$

Although we do not know the oil film thickness h_0, we can estimate how much it is changed by the dynamic responses of the system. If the maximum dynamic load accounts for 5% of the static thrust loads, i.e. F varies from 95% to 105% of the static thrust load, the total oil film thickness will vary within (0.975-1.025) of the initial thickness h_0, i.e. the dynamic responses cause maximum 2.5% change of h_0 which is relatively small. It is reasonable to treat the oil film thickness under steady operational condition as constants where the Lyapunov based estimations apply.

Nevertheless, if there is a need to treat the thickness as a time varying item, the two expressions of equation (23) can be substituted into the system model of equation (13). The addition of nonlinearity can be coped with backstepping control structures. However, in this case, the challenging task is the estimation of the initial thickness h_0 staying in the term of $(h_0 + f(x_h, x_s))^3$. It is typically tedious nonlinear parameter estimation without guaranteed convergence.

PERFORMANCE ANALYSIS

The performance of the controller strongly depends on the design constants k_1~k_4. With different choices of those constants, we investigated their impact on the transient settle time and overshoot of the controller.

6.1 Impact on the bearing house response (x_1, x_2)

Figure 10 clearly illustrates the effect of controller design constants on bearing house response. The constant k_1~k_4 were set to different values between 60 and 6000. With all the cases, the responses can quickly converge to zero without substantially great overshoot. However, it is obvious that the greater the constants are, the faster the convergence is and the smaller the overshoot is. Greater constants at the same time also mean greater control efforts.

The simulations also found when the constants are smaller than 60, the response experiences a large overshoot during transient which will be over the physical mechanical limit of the AMB air gap.

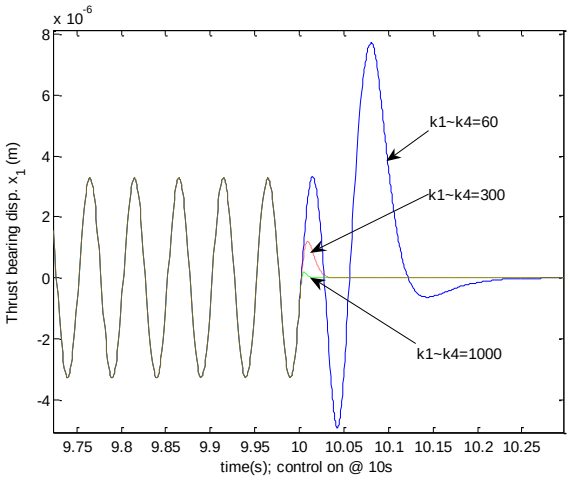

Figure 10 The transient bearing house response under the same control structure with different constants k_1-k_4

6.2 Impact on the shaft response (x_3, x_4)

Shaft response (x_3, x_4) is the zero dynamics of the system, which is equivalently pole-zero cancellation for a linear plant. The impacts of design constants on them are more complex. As an example, we present the results of the case where k_1=k_2 varying from 60 to 6000 and k_3 = k_4 varying from 60 to 6000. It is reasonable to set k_1=k_2 and k_3=k_4 during this application since simulations indicate the design constants k_1 and k_2 for the first two steps can be swapped without obvious impact on the controller performance, and k_3 and k_4 are the two constants for the two identical AMBs in step three. All the results were plotted as contours with Figure 11 and Figure 12 given as the examples of transient settle time and transient overshoot of shaft response.

Observations and comments

a) Figure 11 shows that at small $k_1(k_2)$ =(60-150) and small $k_3(k_4)$=(60-95) area, transient periods of shaft response are very short, the settle times are normally less than 1 second.

b) It can be seen from Figure 12 that in the area with $k_1(k_2)$ =(60-95) and $k_3(k_4)$=(95-950), transient overshoots are large with peak values of more than 15 times of shaft response before control. In high $k_1(k_2)$ area, overshoot ratio is normally less than 10.

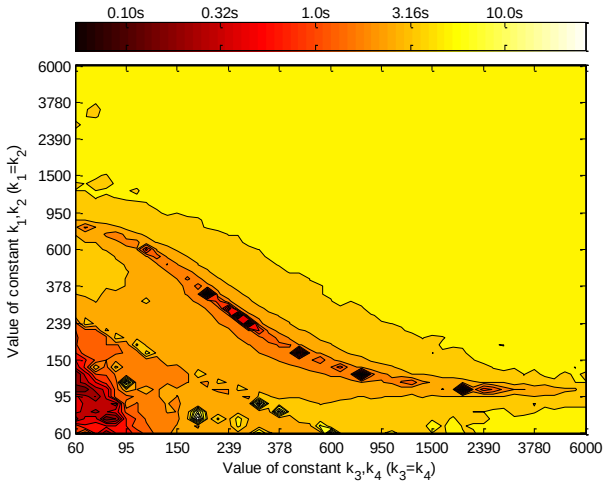

Figure 11 Contour map of transient settle time for shaft response with k_1=k_2=*(60~6000)* & k_3=k_4= *(60~6000)*

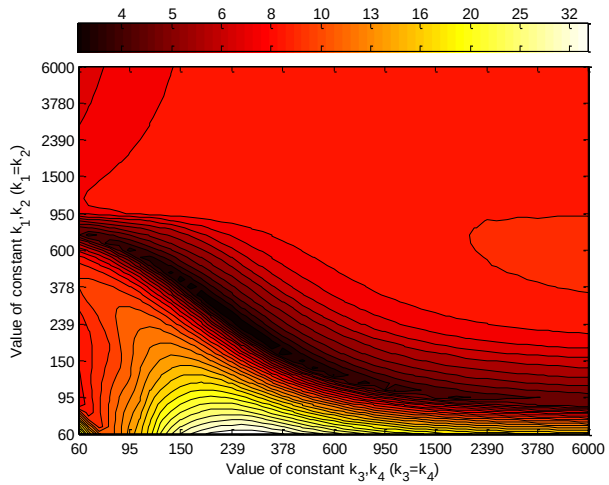

Figure 12 Contour map of transient overshoot for shaft response with $k_1=k_2=(60\sim6000)$ & $k_3=k_4=(60\sim6000)$

6.3 Impact of constant γ_0

γ_0 is the small constant in the force distribution function of the AMBs, its value has impact on the control efforts required. Figure 13 gives the control voltage required at different γ_0 (gama0). Obviously at the switching point, small γ_0 requires much higher capacity from the control system.

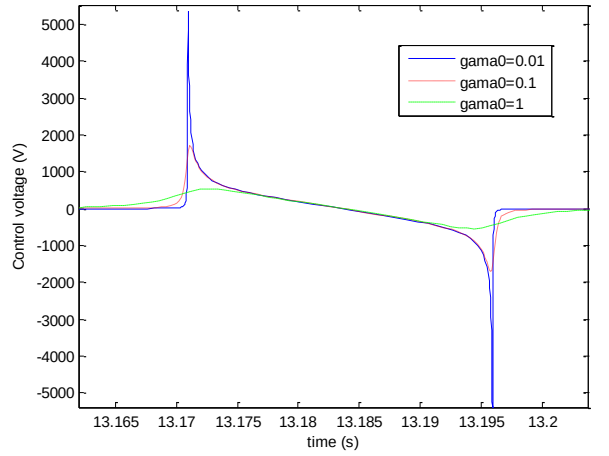

Figure 13 Control voltages required with different value of γ_0 to achieve the control goal

CONCLUSIONS

The comprehensive nonlinear active controller and parameter estimators proposed in this study are stable and robust in minimizing the transmission of propeller induced vibration into the hull structures. This paper summarizes the results of system dynamics, actuator design, controller design, stability analysis and performance analysis.

The system is controllable where dynamic energy can be diverted from thrust bearing house to the shaft. To what extent the shaft response will increase depends on the system configuration. There are possibilities that the shaft responses will be attenuated as well after the control.

With proper AMB force distribution function proposed, the nonlinear controller successfully regulated the bearing house responses (x_1, x_2) to zero. The controlled system is an ISS stable system. The control input is subject to the choice of constant γ_0 in the distribution function.

The estimator is an over-parameterized structure. The adaptive laws work effectively with the nonlinear controller for regulating bearing house responses (x_1, x_2) when parameters uncertainties in presence. Not all unknowns converged to the true value due to inadequate persistent exciting conditions; however, the discrepancy does not prevent the controller from achieving the control goals.

The performance of the nonlinear controller with different design constants was discussed in detail. The impact of different constant choices on the transient settle time, transient overshoot of the bearing house response (x_1, x_2) is straightforward that higher values result in better performance. However, the impacts on those of the shaft response (x_3, x_4) are more complicated. The simulation results show that there are optimal combinations of design constants existing where the controller can reach its best performances.

REFERENCES

Baz,A., Gilheany,J., Steimel,P., 1988, 'Active vibration control of propeller shafts.' *Journal of Sound and Vibration*, pp. 361-372.

Dylejkoa,P.G., Kessissogloua,N.J., Tso,Y., Norwood,C.J., 2007, 'Optimum quasi-adaptive resonance changer for submerged vessel signature reduction.' 2007, *ICSV14 Proceeding*, Cairns.

Goodwin, A.J.H. 1960, 'The design of a resonance changer to overcome excessive axial vibration of propeller shafting.' *Transactions of the institution of marine engineers*,37-78.

Hansen,C., Snyder,S., 1997, *Active Control of Noise and Vibration.* E&FN Spon, London.

Kristic,M., Kanellakopoulos,I., Kokotovic,P. 1995, *Nonlinear and adaptive control design.* John Wiley & Sons, Inc., New York .

Lewis,D., Allaire,P., 1986, 'Control of oscillating transmitted force of axial-thrust bearing with a secondary magnetic bearing.' ASLE, 86-AM-2A-2, *ASLE-REPRINT*, Toronto.

Lewis,M., 1963, 'Propeller vibration forces.' *Transactions of the society of naval architeture and marine engineers*, pp. 293-326.

Liu,W., Pan,J., Mathews,D., 2010, 'Measurement of sound radiation from a torpedo-shaped structure subject to an axial excitation.' *Proceedings of 20th International Congress on Acoustics.* ICA2010, Sydney.

Merz,S., Kessissoglou,N.J., Kinns,R., 2007, 'Excitation of a submarine hull by propeller forces.' *ICSV14*, Cairns.

Ojak,W., 1984, 'Vibration force reducer and a new approach to ship vibration.' *Journal of ship research*, pp.118-140.

Pan,J., Farag,N., Lin,T., Juniper,R., 2002, 'Propeller induced structural vibration through the thrust bearing.' *Proceedings of Acoustics 2002.* Adelaide, pp. 390-399.

Schweitzer,G., Bleuler,H., Traxler, A., 1994, *Active Magnetic Bearings.* vdf Hochschulverlag AG, Zurich.

Storteig,E., White,M., 1999, 'Dynamic characteristics of hydrodynamically lubricated fixed-pad thrust bearings.' *Wear, Vol.232*, 250-255.